

## Chronic Hepatitis C Is Associated With Peripheral Rather Than Hepatic Insulin Resistance

KERRY-LEE MILNER,\* DAVID VAN DER POORTEN,<sup>†</sup> MICHAEL TRENELL,<sup>§</sup> ARTHUR B. JENKINS,<sup>||</sup> AIMIN XU,<sup>¶</sup> GEORGE SMYTHE,<sup>#</sup> GREGORY J. DORE,\*\* AMANY ZEKRY,<sup>‡‡</sup> MARTIN WELTMAN,<sup>§§</sup> VINCENT FRAGOMELI,<sup>§§</sup> JACOB GEORGE,<sup>‡</sup> and DONALD J. CHISHOLM\*

\*Garvan Institute for Medical Research, University of New South Wales, Sydney, Australia; <sup>†</sup>Storr Liver Unit, Westmead Millennium Institute, University of Sydney, Sydney, Australia; <sup>§</sup>Institute of Cellular Medicine, Newcastle University, Newcastle upon Tyne, United Kingdom; <sup>||</sup>School of Health Sciences, University of Wollongong, Wollongong, Australia; <sup>#</sup>Department of Medicine and Pharmacology and Research Center of Heart, Brain, Hormone and Healthy Ageing, University of Hong Kong, Hong Kong, China; <sup>¶</sup>Bioanalytical Mass Spectrometry Facility, University of New South Wales, Sydney, Australia; <sup>\*\*</sup>National Centre in HIV Epidemiology and Clinical Research, University of New South Wales, Sydney, Australia; <sup>‡‡</sup>St George Hospital Clinical School, University of New South Wales, Sydney, Australia; <sup>§§</sup>Department of Gastroenterology and Hepatology, Nepean Hospital and University of Sydney, Western Clinical School, Sydney, Australia

**BACKGROUND & AIMS:** Chronic hepatitis C (CHC) is associated with insulin resistance (IR), liver steatosis (genotype 3), and increased diabetes risk. The site and mechanisms of IR are unclear. **METHODS:** We compared cross-sectionally 29 nonobese, normoglycemic males with CHC (genotypes 1 and 3) to 15 adiposity and age-matched controls using a 2-step hyperinsulinemic-euglycemic clamp with [6,6-<sup>2</sup>H<sub>2</sub>] glucose to assess insulin sensitivity in liver and peripheral tissues and <sup>1</sup>H-magnetic resonance spectroscopy to evaluate liver and intramyocellular lipid. Insulin secretion was assessed after intravenous glucose. **RESULTS:** Insulin secretion was not impaired in CHC. Peripheral insulin sensitivity was 35% higher in controls vs CHC ( $P < .001$ ) during high-dose ( $264.3 \pm 25$  [standard error] mU/L) insulin ( $P < .001$ ); this was negatively associated with viral load ( $R^2 = .12$ ;  $P = .05$ ) and subcutaneous fat ( $R^2 = .41$ ;  $P < .001$ ). IR was similar in both genotypes despite 3-fold increased hepatic fat in genotype 3 ( $P < .001$ ). Hepatic glucose production ( $P = .25$ ) and nonesterified free fatty acid ( $P = .84$ ) suppression with insulin were not different between CHC and controls inferring no adipocyte IR, and suggesting IR is mainly in muscle. In CHC, intramyocellular lipid was nonsignificantly increased but levels of glucagon ( $73.8 \pm 3.6$  vs  $52.8 \pm 3.1$  ng/mL;  $P < .001$ ), soluble tumor necrosis factor receptor 2 ( $3.1 \pm 0.1$  vs  $2.3 \pm 0.1$  ng/mL;  $P < .001$ ), and Lipocalin-2 ( $36.4 \pm 2.9$  vs  $19.6 \pm 1.6$  ng/mL;  $P < .001$ ) were elevated. **CONCLUSIONS:** CHC represents a unique infective/inflammatory model of IR, which is predominantly in muscle, correlates with subcutaneous, not visceral, adiposity, and is independent of liver fat.

**Keywords:** Chronic Hepatitis C; Insulin Resistance; Hyperinsulinemic-Euglycemic Clamp; Liver Steatosis.

View this article's video abstract at [www.gastrojournal.org](http://www.gastrojournal.org).

Chronic hepatitis C (CHC) is of growing concern due to its high prevalence and potential for progression to cirrhosis, liver failure, and hepatocellular carcinoma, but also because of the risk of type 2 diabetes.<sup>1</sup> Patients with CHC and minimal fibrosis are insulin-resistant, measured by homeostasis model assessment (HOMA-IR, based on fasting glucose and insulin measurement), which appears to influence liver disease progression (fibrosis)<sup>2</sup> and treatment outcomes.<sup>3</sup>

The primary sites of insulin action and resistance are muscle, adipose tissue (peripheral compartment), and liver. All studies to date, except two<sup>4,5</sup> quantifying insulin-resistance (IR) in CHC (>100 publications), have utilized HOMA-IR, which is widely used in epidemiological studies and normally accounts for approximately 65% of the variability in insulin sensitivity assessed by hyperinsulinemic clamp,<sup>6</sup> but does not determine hepatic vs peripheral effects. We have used a 2-step hyperinsulinemic-euglycemic clamp (gold standard to measure IR) with tracer glucose infusion to confirm IR and assess whether this is peripheral or hepatic.

Little is known about the mechanisms of IR in CHC and whether it is induced by the virus itself or via an immune/inflammatory response. Systemic low-grade inflammation associated with obesity is linked with IR, type 2 diabetes, and atherosclerosis. CHC infection is associated with up-regulation of Th1 cytokines, particularly tumor necrosis factor  $\alpha$  (TNF- $\alpha$ )<sup>7</sup> and has a high circulating viral load. Postulated mechanisms for IR in CHC include alterations in adipokines and pro-inflam-

**Abbreviations used in this paper:** AFABP, adipocyte fatty acid-binding protein; AUC, area under the curve; BMI, body mass index; CHC, chronic hepatitis C; HCV, hepatitis C virus; EGP, endogenous glucose production; HOMA-IR, homeostasis model assessment of insulin resistance; IL, interleukin; IR, insulin resistance; sTNFR2, soluble tumor necrosis factor receptor 2; TGD, total glucose disposal; TNF- $\alpha$ , tumor necrosis factor  $\alpha$ .

matory cytokines associated with hepatic inflammation, namely reduced adiponectin, increased TNF- $\alpha$ ,<sup>8</sup> and interleukin-6 (IL-6), although we have been unable to demonstrate a virus-specific effect on serum cytokines that could modulate IR<sup>9</sup> or direct interference of hepatitis C virus (HCV) with insulin signaling or lipid synthesis in the liver.<sup>10</sup> Most of these suggested mechanisms would induce hepatic IR, except for viral-induced cytokines, which have systemic effects.

HCV is highly heterogeneous with 6 genotypes. Different genotypes do not differ dramatically in virulence or prognosis, however, vary in responsiveness to antiviral therapy and in deposition of hepatic lipid, with greater hepatic steatosis in genotype 3 infection.<sup>11</sup> There is also a complex interaction of HCV with lipid metabolism that is independent of genotype (including down-regulation of peroxisome proliferator-activated receptor- $\alpha$ <sup>12</sup> and hepatic lipase C and up-regulation of sterol regulatory element binding proteins).<sup>13</sup> We elected to study genotypes 1 and 3 infection as these genotypes are common, have worldwide distribution, and differ substantially in hepatic lipid accumulation. We additionally assessed fat depots in the abdomen, liver, and muscle (using magnetic resonance imaging and spectroscopy), because distribution of fat, especially visceral adiposity, intrahepatic,<sup>14</sup> and intramyocellular lipid,<sup>15</sup> have all been associated with IR.

Thus, the aims of this study were to confirm IR in CHC using the 2-step hyperinsulinemic-euglycemic clamp and to assess the site and correlates of this IR, especially the relationships between adipocytokines, hepatic, abdominal, and myocellular lipid levels and insulin sensitivity.

## Materials and Methods

See additional information regarding methods in the Supplementary Materials and Methods.

### Subjects

Twenty-nine male, nonobese (body mass index [BMI]  $25.7 \pm 3.3 \text{ kg} \cdot \text{m}^{-2}$ ) Caucasian subjects (median age, 40 years; range, 29–53 years) with CHC (the majority with injecting drug use acquired infection) genotypes 1 ( $n = 15$ ) or 3 ( $n = 14$ ), due to start antiviral therapy at 4 different hospital clinics were recruited to the study between 2005 and 2008. To minimize impact of known determinants of insulin resistance, inclusion criteria were (1) BMI  $<30 \text{ kg} \cdot \text{m}^{-2}$ ; (2) fasting blood glucose level  $<5.5 \text{ mmol/L}$ ; (3) absent or minimal fibrosis (fibrosis score  $\leq F2$ ) on liver biopsy (23 subjects [79%] had a liver biopsy) or a Fibrosis Probability Index score  $\leq 0.3$ <sup>16</sup> and Forns index  $<6.9$ <sup>17</sup>; and (4) male gender and Caucasian background. Fifteen healthy HCV antibody-negative controls recruited from the community (median age 37 years) with normal liver function tests were matched by age, ethnicity, gender, and BMI to the subjects mentioned previously. Patients with alcohol consumption  $>20 \text{ g}$  per

day were excluded (assessed by 2 separate interviews with patient and family). Other exclusion criteria included concurrent HIV or other causes of liver disease. This study had 80% power to detect a difference in glucose infusion rate (measure of IR) of  $3 \text{ mg} \cdot \text{kg}^{-1} \cdot \text{min}^{-1}$  between groups containing 15 subjects each, assuming a common standard deviation of 2.8. All examinations were undertaken after a 10-hour fast following abstinence of strenuous exercise and alcohol or use of addictive drugs for 48 hours prior to the study. Those on methadone could continue their normal dosing regime. Routine physical activity was assessed by a standardized validated questionnaire<sup>18</sup> calculating average weekly energy expenditure. Dietary composition and energy intake were measured by a detailed dietary history based on 24-hour recall<sup>19</sup> and quantified using a standard food composition program (Foodworks; Xyris Software, Australia). Protocols were approved by institutional human research ethics committees and all subjects provided written informed consent.

### Histopathology

Twenty-three subjects had a liver biopsy as part of CHC management and degree of necroinflammatory activity and fibrosis scored as described by Scheuer.<sup>20</sup>

### Magnetic Resonance Spectroscopy and Imaging

<sup>1</sup>H-NMR spectroscopy of hepatic<sup>21</sup> and intramyocellular<sup>22</sup> triglyceride content and abdominal magnetic resonance imaging for assessment of subcutaneous and visceral fat were performed on a 1.5-Tesla scanner (General Electric Medical Systems, Milwaukee, WI).<sup>23</sup>

### Baseline Assessment and Anthropometry

Following imaging, weight, height, and waist circumference were measured and BMI was calculated as weight (in kilograms) divided by height (meters) squared and waist-to-hip ratio by dividing waist by hip circumference. Blood pressure was measured supine after a 5-minute rest. Blood was collected for analytes indicated here.

### Intravenous Glucose Tolerance Test

Teflon catheters were placed in the antecubital vein for infusions and into a contralateral dorsal hand vein, heated using a warming device placed over the arm and hand to achieve arterialization of venous blood, for blood sampling. A small volume of normal saline (0.9%) was infused in both lines to maintain patency. An intravenous glucose tolerance test was performed, to assess beta ( $\beta$ ) cell function, with a bolus of 50% dextrose (300 mg/kg, maximum 24 g) administered intravenously for 1 minute and glucose (YSI 2300 Stat Plus; Yellow Springs Instruments, Yellow Springs, OH) and insulin levels measured for 10 minutes. The acute insulin response was

calculated as the ratio of the increment of serum insulin (mU/L) to that of blood glucose (mmol/L) during the 10 minutes of the intravenous glucose tolerance test. The incremental insulin (AUC<sub>insulin</sub>) and glucose (AUC<sub>glucose</sub>) areas under the curve were calculated by the trapezoidal method.

### *Hyperinsulinemic-Euglycemic Clamp*

This was performed using a 2-hour primed (5 mg · kg<sup>-1</sup> body weight), continuous (3 mg · kg<sup>-1</sup> · hr<sup>-1</sup>) infusion of [6,6-<sup>2</sup>H<sub>2</sub>] glucose (to estimate both endogenous glucose output and peripheral disposal) using a low-dose (15 mU · m<sup>-2</sup> · min<sup>-1</sup>) and high-dose (80 mU · m<sup>-2</sup> · min<sup>-1</sup>) insulin infusion, over 90 and 120 minutes, respectively.<sup>24,25</sup> The plasma glucose level was maintained at 5 mmol/L with a variable-rate infusion of dextrose (25 g/100 mL enriched to approximately 2.5% with di-deuterated glucose) adjusted according to 10-minute results. [6,6-<sup>2</sup>H<sub>2</sub>] Glucose infusion was ceased 10 minutes after the commencement of the [6,6-<sup>2</sup>H<sub>2</sub>] glucose-enriched dextrose. Five subjects (3 controls and 2 CHC subjects) did not receive this enhanced [6,6-<sup>2</sup>H<sub>2</sub>] glucose delivery during hyperinsulinemia and are not included in glucose turnover studies during the hyperinsulinemia, although basal turnover and clamp glucose infusion rate are reliable and included in the results. One control subject did not attain steady-state during low-dose insulin. Thus, numbers for basal glucose turnover data are control 15, CHC 29. For the clamp low-dose insulin (and for calculations of low insulin vs basal), the numbers are control 11, CHC 27. The coefficient of variation for the glucose levels at the low- and high-dose insulin was 2.66% and 3.98%, respectively. The [6,6-<sup>2</sup>H<sub>2</sub>] glucose enrichment in serum samples was measured by gas chromatography-mass spectrometry.<sup>26</sup> The coefficient of variation for deuterated glucose measurements at the low- and high-dose insulin was 4.8% and 3.7%, respectively. The steady-state glucose infusion rate (M value) represented net whole-body glucose disposal, an estimate of insulin sensitivity and was calculated as a mean at 10-minute intervals during the last 40 minutes of the low- and high-dose insulin clamp. Blood samples were also drawn at these intervals for insulin, glucagon (frozen with trasylol), c-peptide, and glucose isotope enrichment.

### *Calorimetry*

During the final 30 minutes of the basal infusion and each step of the clamp, indirect calorimetry was performed using the ventilated hood technique (Deltatrack Metabolic Monitor; Datex Instrumentarium, Helsinki, Finland) to measure basal fasting and insulin stimulated glucose and fat oxidation as described previously.<sup>27</sup>

### *Analyses*

Serum insulin, glucagon, adiponectin, c-peptide, leptin, TNF- $\alpha$ , soluble tumor necrosis factor receptor 2

(sTNFR2), adipocyte fatty acid-binding protein (AFABP), Lipocalin-2, and IL-6 were measured by sandwich enzyme-linked immunosorbent assay; nonesterified free fatty acids by an enzymatic colorimetric method; highly sensitive C-reactive protein by a highly sensitive immunoassay; lipid and liver function tests were performed using a conventional automated analyzer; viral load or HCV RNA was measured by the polymerase chain reaction method; HCV genotype by second generation reverse hybridization line probe assay and HCV antibodies by enzyme-linked immunoassay.

### *Calculations*

Isotopic enrichment determined by gas chromatography-mass spectrometry was corrected for the constant background contribution of naturally occurring [6,6-<sup>2</sup>H<sub>2</sub>] glucose, and the values obtained were smoothed by linear regression against time within each measurement period.<sup>28</sup> The rates of endogenous glucose production (EGP) and total glucose disposal (TGD) were estimated during the basal and insulin-stimulated 30-minute steady-state periods using Steele's 1-compartment fixed-volume model (assuming a pool-fraction of 0.65 and a volume of distribution of 20% of body weight),<sup>29</sup> as modified by Finegood et al<sup>30</sup> to account for the added infusion of labeled exogenous glucose.

### *Statistical Analysis*

Statistical analysis was carried out using SPSS version 15.0 (SPSS Inc, Chicago, IL). Two-tailed tests with a significance level of 5% were used throughout. Variables exhibiting skewed distribution were log (ln) transformed to approximate normality prior to analysis. For comparison between groups 2-sample Student *t* tests were used for normally distributed variables and the Mann-Whitney *U* test otherwise. Chi-square or Fishers exact tests were used to compare distribution of categorical variables by group. Strength of association between continuous variables was quantified using Spearman rank correlations. Linear models were used to examine univariate relationships between IR and continuous variables of interest. Stepwise multiple linear regression identified the independent predictors of insulin resistance. Subjects with missing data were excluded on analysis by analysis basis. Repeated measures analysis of variance analyzed the relationship between the effects of subject factor and group on variables of interest. Data are expressed as the mean  $\pm$  standard deviation in the text.

## **Results**

### *Baseline Characteristics of Subjects*

CHC subjects (n = 29) and controls (n = 15) were selected to be matched for age, weight, BMI, and were

**Table 1.** Baseline Characteristics of Study Cohort

	Control (n = 15)	CHC (n = 29)	P value <sup>a</sup>	G1 (n = 15)	G3 (n = 14)	P value <sup>b</sup>
Age (y)	37.40 (6.6)	40.48 (6)	.13	40.7 (4.8)	40.3 (7.2)	.9
BMI (kg/m <sup>2</sup> )	25.2 (2.6)	25.7 (3.3)	.63	26.2 (3)	25.2 (3.6)	.4
Waist (cm)	89.5 (7.1)	90.4 (7.8)	.71	90.2 (5.3)	90.7 (10.1)	.9
WHR	0.92 (0.1)	0.94 (0.1)	.16	0.94 (0.03)	0.94 (0.06)	.8
Blood pressure (mm Hg)	116/75	117/78	>.3	116/78	119/78	>.3
Subcut fat volume (kg) <sup>c</sup>	6.7 (2.7) <sup>d</sup>	7.2 (3.3)	.8	7.3 (3.1)	7.04 (3.6)	.6
Visceral fat volume (kg) <sup>c</sup>	3.3 (1.8) <sup>d</sup>	3.5 (1.9)	.8	3.2 (1.2)	3.8 (2.4)	.95
Smokers, n (%)	1 (7)	21 (72)	<.001	10 (67)	11 (79)	.7
Methadone users, n (%)	0 (0)	6 (20.7)	.08	3 (20)	3 (21)	.99
FH T2DM, n (%)	8 (53.3)	13 (44.8)	NS	7 (47)	4 (29)	.5
Alcohol intake (g/wk)	49	33	NS	40	27	.2
Fasting glucose (mmol/L)	4.56 (0.3)	4.6 (0.4)	.8	4.7 (0.5)	4.5 (0.3)	.5
Fasting insulin (mU/L) <sup>c</sup>	8.3 (2.7)	11.5 (4.8)	.04	11.8 (5.2)	11.2 (4.6)	.7
HOMA-IR <sup>c</sup>	1.7 (0.6)	2.4 (1.1)	.05	2.5 (1.2)	2.3 (1.03)	.6
Glucagon (ng/mL) <sup>c</sup>	52.8 (12)	73.8 (19.2)	<.001	71 (11.3)	76.8 (25.3)	.6
C-peptide (mmol/L) <sup>c</sup>	3.1 (1.3) <sup>d</sup>	4.6 (2.3)	.02	5 (1.7)	4.1 (2.8)	.1
Cholesterol (mmol/L)	4.8 (1)	4.1 (1.1)	.04	4.5 (1)	3.6 (1)	.02
LDL (mmol/L)	3.0 (0.9)	2.4 (0.9)	.03	2.6 (0.9) <sup>d</sup>	2.14 (0.7)	.1
Triglycerides (mmol/L) <sup>c</sup>	0.97 (0.5)	1.02 (0.4)	.5	1.2 (0.4)	0.8 (0.3)	.002
HDL (mmol/L)	1.4 (0.3)	1.2 (0.3)	.11	1.3 (0.3) <sup>d</sup>	1.1 (0.3)	.2
NEFA (mmol/L) <sup>c</sup>	0.4 (0.2)	0.5 (0.2)	.1	0.5 (0.2)	0.6 (0.2)	.3
ALT (U/L) <sup>c</sup>	20.7 (5.5)	91.5 (69.3)	<.001	69.7 (22.3)	61.6 (29)	.02
Adiponectin (ug/mL)	9.9 (5.5)	13.7 (7.1)	.09	12.3 (6.8)	15.1 (7.5)	.3
Leptin (ng/mL) <sup>c</sup>	9.4 (3.6)	12.3 (6.9)	.2	11.8 (8.3)	12.8 (5.4)	.3
sTNFR2 (ng/mL)	2.3 (0.6)	3.1 (0.4)	<.001	3 (0.4)	3.3 (0.4)	.052
TNF-α (pg/mL) <sup>c</sup>	2.9 (1.7)	4.1 (2.1)	.02	4.2 (2.3)	4 (2)	.9
IL-6 (pg/mL) <sup>c</sup>	1.5 (0.5)	2.6 (2.1)	.08	2.4 (1.9)	2.8 (2.3)	.9
CRP (mg/L) <sup>c</sup>	0.8 (0.8)	1.3 (1.6)	.3	0.9 (1.1)	1.7 (2)	.2
Lipocalin-2 (ng/mL) <sup>c</sup>	20.4 (6.4)	36.4 (15.5) <sup>d</sup>	<.001	37.5 (13.3) <sup>d</sup>	35.4 (18)	.5
AFABP (ng/mL) <sup>c</sup>	14.0 (4.2)	16.8 (6.8) <sup>d</sup>	.2	16.5 (7.6) <sup>d</sup>	17.1 (6)	.6
Viral load (IU/mL) <sup>c</sup>	—	1,789,475 (2,260,309)	—	2,282,063 (770,797) <sup>d</sup>	1,214,789 (304,431) <sup>e</sup>	.49

NOTE. Results expressed as mean (standard deviation) or frequency (percentage).

ALT, alanine aminotransferase; FH T2DM, family history of type 2 diabetes; G1, genotype 1; G3, genotype 3; HDL, high-density lipoprotein; LDL, low-density lipoprotein; NEFA, nonesterified free fatty acids; NS, not significant; subcut, subcutaneous; WHR, waist-to-hip ratio.

<sup>a</sup>P value between hepatitis C and control subjects.

<sup>b</sup>P value between genotypes 1 and 3.

<sup>c</sup>These have been log transformed (Ln) prior to analysis (skewed distribution).

<sup>d</sup>Data missing in 1 subject.

<sup>e</sup>Data missing in 2 subjects.

similar for abdominal fat (visceral and subcutaneous fat). There was a higher frequency of smokers and methadone users in CHC subjects (Table 1). Among CHC subjects, methadone users and smokers, compared to nonusers, had similar baseline characteristics except for higher waist-to-hip ratios ( $P = .04$ ) in methadone users and higher highly sensitive C-reactive protein ( $P = .02$ ) and low-density lipoprotein ( $P = .02$ ) in smokers. Both groups had similar frequency of family history of type 2 diabetes. CHC subjects had higher baseline alanine aminotransferase. All baseline characteristics were the same between genotypes 1 and 3 except alanine aminotransferase ( $P = .01$ ) and gamma-glutamyl transferase ( $P = .04$ ) were higher in genotype 3. Alcohol intake was not significantly higher in controls ( $P = .25$ ). There was no difference in macronutrient consumption or physical activity between CHC and control subjects (data not shown).

**Baseline Glucoregulatory Hormones and Lipids**

CHC subjects and controls had similar fasting plasma glucose but insulin, c-peptide, and HOMA-IR levels were higher in CHC (Table 1). Triglycerides, non-esterified free fatty acids and high-density lipoprotein were similar in both groups; however, total cholesterol and low-density lipoprotein were lower in CHC as reported previously.<sup>31</sup> Fasting glucagon levels were increased in CHC vs controls ( $73.8 \pm 19.2$  vs  $52.8 \pm 12.0$  ng/mL;  $P < .001$ ). There were no genotype differences except fasting cholesterol ( $P = .02$ ) and triglycerides ( $P = .004$ ) were lower in genotype 3.

**Intravenous Glucose Tolerance Test**

Post glucose load, insulin levels tended to be higher in CHC (Figure 1A), but were not significantly different from controls for AUC insulin or acute insulin

CLINICAL-LIVER, PANCREAS, AND BILIARY TRACT

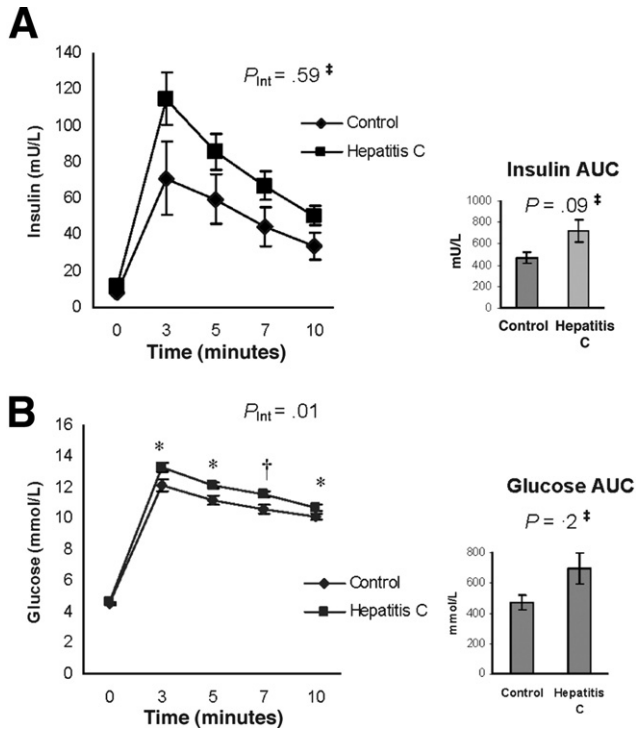


**Figure 1.** Mean ( $\pm$  standard error) serum concentrations of insulin (A) and glucose (B) during an intravenous tolerance test between hepatitis C subjects and controls. \* $P < .05$ ;  $\ddagger P < .01$ ;  $\ddagger$ Data log transformed (Ln) prior to analysis.

response. Glucose levels (Figure 1B) were higher in CHC at 3, 5, 7, and 10 minutes but AUC ( $P = .2$ ) and incremental AUC ( $P = .3$ ) for glucose were not significantly different from controls. There were no differences between genotypes.

### Hyperinsulinemic-Euglycemic Clamp

Basal rates of EGP were significantly lower in the CHC subjects ( $n = 29$ ) compared to controls ( $n = 15$ ) ( $1.5 \pm 0.5$  vs  $1.9 \pm 0.6$   $\text{mg} \cdot \text{kg}^{-1} \cdot \text{min}^{-1}$ ;  $P = .04$ ). The basal hepatic insulin resistance index (EGP  $\times$  fasting insulin) is similar in the CHC subjects compared to the controls (controls  $15.9 \pm 9$ , CHC  $17.3 \pm 9.3$   $\text{mg} \cdot \text{mU} \cdot \text{kg}^{-1} \cdot \text{min}^{-1} \cdot \text{L}^{-1}$ ;  $P = .56$ ). EGP suppressed during low-dose insulin by 65% in CHC ( $n = 27$ ) and 80% in controls ( $n = 11$ ) ( $P = .25$ ) (to  $0.55 \pm 0.5$  vs  $0.5 \pm 0.9$   $\text{mg} \cdot \text{kg}^{-1} \cdot \text{min}^{-1}$ ;  $P = .85$ ) (Figure 2A). At high-dose insulin, EGP was completely suppressed (levels not significantly different from 0).

Steady-state insulin levels increased during the clamp in CHC subjects and controls to  $35 \pm 6.8$  and  $30.4 \pm 6.4$   $\text{mU/L}$  ( $P = .04$ ) at low-dose and to  $276.4 \pm 184$  and  $240.9 \pm 130.8$   $\text{mU/L}$  ( $P = .6$ ) at high-dose, respectively. Glucose infusion rates (M) were 39% higher at low-dose and 35% higher at high-dose insulin in controls compared to CHC (low-dose  $3.9 \pm 1.2$  vs  $2.8 \pm 1.1$   $\text{mg} \cdot \text{kg}^{-1} \cdot \text{min}^{-1}$ ;  $P = .006$ ; high-dose  $12.8 \pm 2.8$  vs  $9.5 \pm 1.9$   $\text{mg} \cdot \text{kg}^{-1} \cdot \text{min}^{-1}$ ;  $P = .001$ ). M remained significantly

higher in controls when corrected for clamp insulin levels (M/I: low-dose  $0.14 \pm 0.06$  vs  $0.08 \pm 0.03$   $\text{mg} \cdot \text{kg}^{-1} \cdot \text{min}^{-1}$ ;  $P = .001$ ; high-dose  $0.07 \pm 0.04$  vs  $0.04 \pm 0.02$   $\text{mg} \cdot \text{kg}^{-1} \cdot \text{min}^{-1} \cdot \text{L} \cdot \text{mU}^{-1}$ ;  $P = .03$ ) (Figure 2B). If lean mass is estimated from weight and height,<sup>32</sup> glucose infusion rates corrected for fat-free mass still remain higher in the controls compared to CHC (low-dose  $5.36 \pm 1.6$  vs  $3.87 \pm 1.4$   $\text{mg} \cdot \text{kg}$  fat-free mass $^{-1} \cdot \text{min}^{-1}$ ;  $P = .002$ ; high-dose  $17.75 \pm 3.7$  vs  $13.29 \pm 2.2$   $\text{mg} \cdot \text{kg}$  fat-free mass $^{-1} \cdot \text{min}^{-1}$ ;  $P < .001$ ). As EGP was not suppressed at low-dose insulin, TGD is the sum of the M value and EGP. TGD was not significantly different between the control and CHC subjects ( $4.6 \pm 2$   $\text{mg} \cdot \text{kg}^{-1} \cdot \text{min}^{-1}$  vs  $3.3 \pm 0.9$   $\text{mg} \cdot \text{kg}^{-1} \cdot \text{min}^{-1}$ ;  $P = .2$ ). At high-dose insulin, the M value closely approximates TGD as EGP was completely suppressed. There were no genotype differences in glucose infusion rates or total glucose disposal.

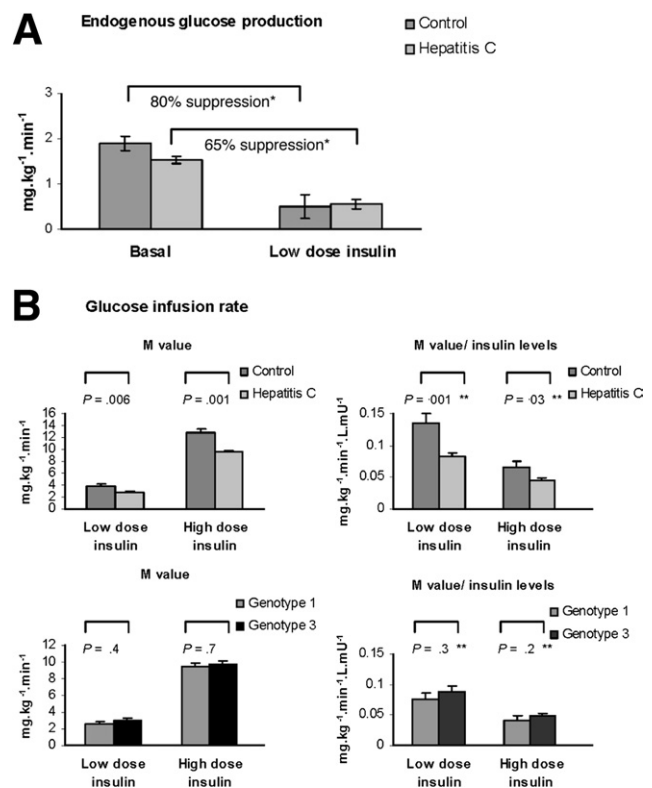


**Figure 2.** Mean ( $\pm$  standard error) endogenous glucose production (A) and exogenous glucose infusion rate (M value and M value/insulin levels) (B) during hyperinsulinemic-euglycemic clamp study in hepatitis C subjects and controls and genotype 1 and 3. \* $P < .001$ ; \*\*These have been log transformed (Ln) prior to analysis. EGP data presented in 11 controls and 27 CHC subjects. M value at low-dose insulin presented in 14 controls and 29 CHC subjects, M value at high-dose insulin presented in 15 controls and 29 CHC subjects.  $P = .25$  (NS) for % suppression EGP in controls vs chronic hepatitis C subjects. Basal EGP significantly lower in hepatitis C subjects compared to controls ( $P = .04$ ), but not significantly different at low-dose insulin clamp ( $P = .85$ ). EGP at high-dose insulin not shown as was not significantly different from zero in all groups.

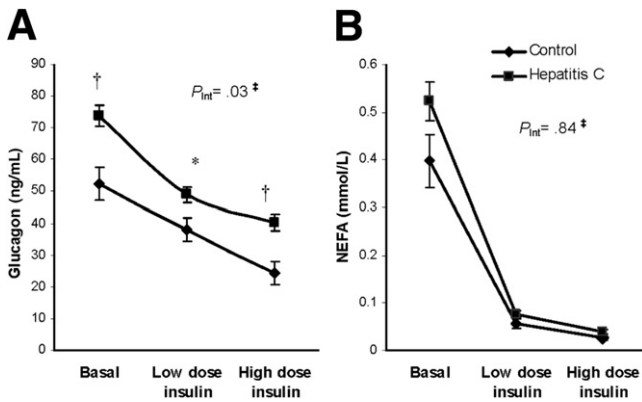


**Figure 3.** Mean ( $\pm$  standard error) serum glucagon (A) and nonesterified free fatty acids (NEFA) (B) levels during hyperinsulinemic-euglycemic clamp in hepatitis C subjects and controls. \* $P < .05$ ; † $P < .01$ ; ‡Data log transformed (Ln) prior to analysis.

CHC smokers ( $n = 21$ ) and nonsmokers ( $n = 8$ ) had similar glucose infusion rates to maintain glycemia at low-dose ( $P = .87$ ) or high-dose ( $P = .84$ ) insulin. Glucose infusion rates in CHC subjects at low-dose insulin were higher in methadone users compared to nonmethadone users ( $4 \pm 1.5$  vs  $2.5 \pm 0.7$   $\text{mg} \cdot \text{kg}^{-1} \cdot \text{min}^{-1}$ ;  $P = .002$ ) and nonsignificantly so at high-dose insulin ( $P = .14$ ). If methadone users and smokers were excluded from analysis, glucose infusion rates at high-dose insulin remained significantly higher in controls vs CHC ( $12.8 \pm 2.8$  vs  $9.3 \pm 1.9$   $\text{mg} \cdot \text{kg}^{-1} \cdot \text{min}^{-1}$ ;  $P < .001$ ;  $12.7 \pm 2.9$  vs  $9.5 \pm 1.96$   $\text{mg} \cdot \text{kg}^{-1} \cdot \text{min}^{-1}$ ;  $P = .01$ , respectively). Additionally, the difference in glucose infusion rate at high-dose insulin between controls and CHC subjects adjusted for methadone, smoking, and family history of type 2 diabetes was  $3.9$   $\text{mg} \cdot \text{kg}^{-1} \cdot \text{min}^{-1}$  (95% confidence interval:  $1.9$ – $5.8$ ;  $P < .001$ ). Glucose infusion rates were comparable in those with and without family history of type 2 diabetes.

Glucagon levels were elevated in CHC compared to control subjects at baseline ( $P < .001$ ) and during hyperinsulinemia ( $P = .03$  low-dose insulin and  $P < .001$  high-dose) and were suppressed at low-dose insulin by 34% and 28% and at high-dose by 46% and 54%, respectively (Figure 3A). Although c-peptide levels were higher

at baseline ( $P = .02$ ) in CHC, levels were suppressed during high-dose insulin by 21% in controls and 30% in CHC subjects. Nonesterified free fatty acid levels tended to be higher at baseline in CHC ( $P = .096$ ), but suppressed similarly (by 85% with low-dose insulin and (by 93%) with high-dose (Figure 3B).

There were no significant differences in fasting and low-dose insulin-stimulated rates of glucose and fat oxidation; however, at high-dose insulin, rates of glucose oxidation ( $P = .02$ ) and nonoxidative glucose metabolism ( $P = .002$ ) were significantly higher in controls than CHC subjects and fat oxidation tended to be higher in CHC subjects ( $P = .06$ ). Whole-body energy expenditure was similar in both groups at rest and with insulin stimulation.

On univariate analysis (adjusted for smoking and methadone use) there was a negative association of peripheral insulin sensitivity (M value at high-dose insulin) with adiposity (BMI, waist circumference, leptin levels) and, interestingly, with subcutaneous but not visceral abdominal fat in CHC. The independent predictors of insulin sensitivity were HCV viral load and subcutaneous fat (both log transformed) (Table 2, Figure 4). In this cohort, measures of IR by clamp had a relatively poor correlation with HOMA-IR ( $r = -0.49$ ;  $P = .008$ ). HOMA-IR was negatively associated with glucagon/insulin ratio ( $r = -0.76$ ;  $P < .001$ ).

**Viral Load**

HCV viral load was not significantly higher in genotype 1 than genotype 3 ( $P = .4$ ) and was negatively associated with the glucose infusion rate at high-dose insulin ( $r = -0.45$ ;  $P = .05$ ) (Figure 4) and positively with portal inflammation (in 17 subjects with liver biopsy) ( $r = 0.572$ ;  $P = .02$ ).

**Adipocytokines**

TNF- $\alpha$ , sTNFR2, and Lipocalin-2 were significantly higher in CHC compared to controls, while IL-6 tended to be higher; leptin, adiponectin, and AFABP levels were not significantly different (Table 1). Leptin, but no other measured adipokine, predicted insulin sensitivity (high-dose insulin  $r = -0.39$ ;  $P = .04$ ) in CHC.

**Table 2.** Factors Associated With Peripheral Insulin Resistance at High-Dose Insulin (M Value) in Univariate and Multivariate Models Adjusted for Smoking and Methadone Use in Chronic Hepatitis C Subjects

	Univariate results				Best fitting multivariate model		
	$\beta$	SE	Adj $r^2$	P value	$\beta$	SE	P adjusted
In subcut fat (kg)	-2.37	0.55	0.41	<.001	-2.5	0.48	<.001
In viral load (IU/mL)	-.48	0.25	0.17	.07	-.6	0.17	.002
Age (y)	-.12	0.06	0.11	.07			
BMI ( $\text{mg} \cdot \text{kg}^{-2}$ )	-.36	0.09	0.38	<.001			
In c-peptide (mmol/L)	-2.2	0.64	0.3	.002			
In leptin (ng/mL)	-1.4	0.61	0.15	.03			

SE, standard error; subcut, subcutaneous (abdominal).

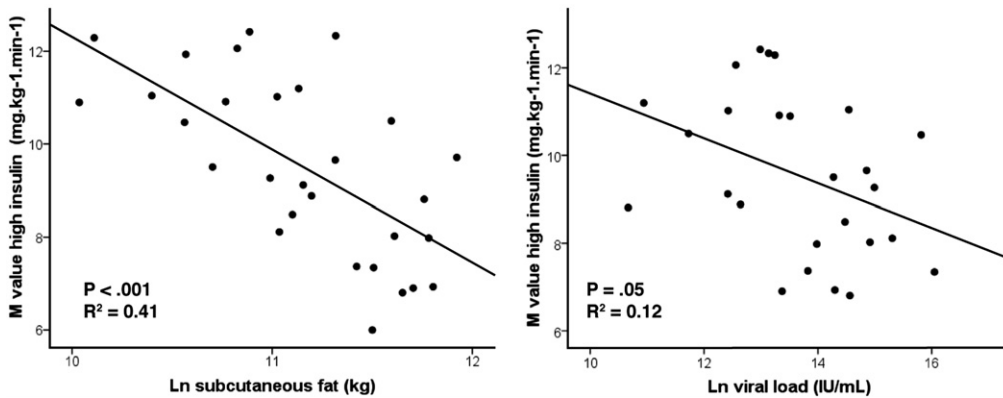


**Figure 4.** Correlation of insulin resistance (M value – high-dose insulin) with hepatitis C viral load and subcutaneous fat (both log transformed) in hepatitis C subjects. Results not adjusted for smoking and methadone use. For adjusted analyses, see Table 2.

### Intramyocellular and Intrahepatic Triglyceride Content

Intramyocellular lipid was not significantly different in CHC subjects and controls ( $2.7 \pm 1.2$  vs  $2.1 \pm 0.6$  mM/kg wet weight;  $P = .13$ ) whereas intrahepatic triglyceride content was significantly higher in CHC compared to controls ( $10.2 \pm 10.1$  vs  $4.5 \pm 2.1$  F/[F+H<sub>2</sub>O]%;  $P = .046$ )—the greater intrahepatic triglyceride content in the CHC subjects can all be accounted for by the elevated intrahepatic triglyceride in genotype 3 (compared to genotype 1;  $15.9 \pm 3.2$  vs  $4.9 \pm 2.9$  F/[F + H<sub>2</sub>O]%;  $P = .003$ ) (Figure 5). There was no difference in intrahepatic triglyceride between controls and genotype 1 ( $4.5 \pm 2.1$  vs  $4.9 \pm 2.9$  F/[F + H<sub>2</sub>O]%;  $P = .9$ ). Genotype 3 had similar intramyocellular lipid content compared to genotype 1 ( $2.6 \pm 1.1$  vs  $2.8 \pm 1.3$  mM/kg wet weight;  $P = .6$ ). In CHC, intramyocellular lipid was associated with HOMA-IR ( $r = 0.38$ ;  $P = .04$ ), leptin ( $r = 0.48$ ;  $P = .009$ ), and M/I high-dose insulin ( $r = -0.49$ ;  $P = .007$ ); liver fat was negatively associated with low-density lipoprotein ( $r = -0.46$ ;  $P = .01$ ) and cholesterol ( $r = -0.38$ ;  $P = .04$ ) and there was no correlation with insulin resistance or suppression of EGP.

### Discussion

This study demonstrates that nonobese male subjects with CHC and mild liver disease had significant IR

compared to healthy controls of similar age, BMI, and physical activity and that this IR is principally in the periphery, contrasting with previous suggestions of impaired hepatic insulin action,<sup>33</sup> although there may be a small contribution from the liver. This observation is supported by the decreased insulin stimulated glucose disposal at high insulin dose clamp (when endogenous glucose production is completely suppressed) and no significant difference in insulin-stimulated hepatic glucose output between CHC subjects and controls at low-dose insulin. If one assumed that the suppression of hepatic glucose output at the lower insulin dose was a true difference between CHC and controls, this would only account for 34% of the difference in insulin-induced net glucose disposal at low-dose and none of the difference at high-dose insulin. This finding of IR predominantly in muscle is consistent with data in a recent paper by Vanni et al<sup>5</sup> where total clamp glucose disposal (using a different insulin dose) was significantly higher in controls compared to CHC subjects, indicative of an approximate 80% peripheral contribution to the IR, even though the authors did not reach this specific conclusion.

There has been increasing evidence of the importance of  $\beta$ -cell failure in development of type 2 diabetes, so it is important that specific testing of insulin secretion showed no suggestion of impaired  $\beta$ -cell function in hepatitis C. In fact there was a nonsignificant tendency to increased insulin levels, compatible with a  $\beta$ -cell response to insulin resistance.

The 2 HCV genotypes studied differ markedly in hepatic steatosis. Despite substantially increased hepatic steatosis in genotype 3, IR was similar in the 2 genotypes suggesting that in this paradigm of IR, hepatic steatosis of a degree similar to that commonly seen in type 2 diabetes is not a significant factor in the IR.<sup>34</sup> Interestingly, in genotype 3, circulating triglycerides were not elevated in the presence of marked hepatic steatosis, which seems to represent a “locking in” of triglycerides in the liver (perhaps via downregulation of microsomal triglyceride transfer protein)<sup>35</sup> and may explain the lack of additional IR in genotype 3.

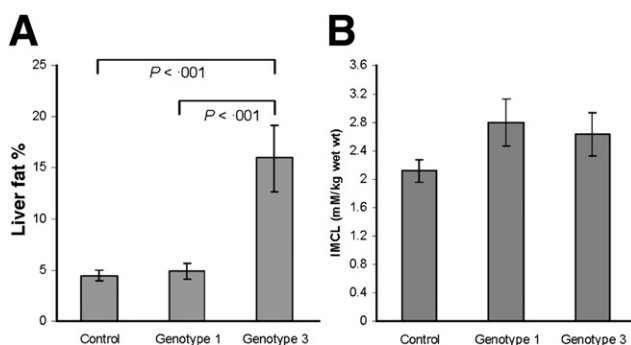


**Figure 5.** Liver (A) and muscle (intramyocellular [IMCL]) (B) fat in controls, genotype 1 and 3 subjects. Data expressed as mean  $\pm$  standard error and log transformed (Ln) prior to analysis.

Free fatty acids tended to be higher in CHC basally, but were suppressed similarly to controls during low-dose insulin. This suggests IR is largely confined to skeletal muscle and not adipose tissue. Intramyocellular lipid content was 22% higher in CHC; this was not significant, but cannot be excluded as a contributor to impaired insulin action in muscle. In fact, there was a significant correlation between intramyocellular lipid in CHC and M/I at high-dose insulin. Furthermore, intramyocellular lipid may not necessarily reflect active lipid metabolites in muscle, such as long-chain fatty acyl CoAs or ceramides, which impede insulin signaling.<sup>36</sup> Other possible mechanisms for IR in skeletal muscle include viral-induced adipocytokine release or HCV viral proteins directly interfering with muscle insulin signaling or inflammatory pathways. It is not known if HCV invades muscle although one study found no evidence of viral replication in skeletal muscle.<sup>37</sup> Insulin sensitivity improves following antiviral therapy<sup>38</sup> consistent with the suggestion that IR is mediated primarily or secondarily by the virus. Peripheral IR in hepatitis C was independently associated with viral load and subcutaneous fat suggesting interplay between the virus itself and peripheral fat stores. The association between IR (using HOMA-IR) and HCV RNA levels was recently reported<sup>39</sup>; however, no studies to date have assessed the relation of different abdominal fat depots to IR in CHC. Visceral fat has been strongly associated with IR and metabolic syndrome variables by our own<sup>40</sup> and other groups but in our study there was no correlation between IR and visceral fat in CHC; rather an unusually strong correlation with subcutaneous fat.

Adipocytokines play a role in development of obesity-related IR,<sup>41</sup> especially adiponectin. Reduced adiponectin has been associated with insulin resistance, steatosis, and inflammation.<sup>42</sup> In our study, adiponectin and leptin levels were similar in CHC and controls and did not predict IR on multivariate analysis. This agrees with our recent report<sup>9</sup> that males with hepatitis C and early liver disease had similar adiponectin and leptin levels to age- and BMI-matched controls. In addition, there were no associations between these adipokines and histological markers of disease severity. As shown previously,<sup>7</sup> circulating levels of the inflammatory cytokines TNF- $\alpha$  and sTNFR2 (reflecting TNF- $\alpha$  activity) were elevated in CHC. Although these cytokines are associated with peripheral IR,<sup>43,44</sup> in our study levels did not correlate with insulin action, suggesting a secondary mechanism in IR. This is further substantiated by the lack of IR in chronic hepatitis B infection, where TNF- $\alpha$  levels are also elevated.

Lipocalin-2 and AFABP levels have not previously been reported in CHC. Lipocalin-2, a protein/adipokine with diverse functions and abundantly expressed in many tissues, including the liver, macrophages, and adipose tissue, has been implicated in the development of obesity-related inflammation and IR.<sup>45</sup> Lipocalin-2 levels were 46% higher in CHC compared to controls and were as-

sociated with TNF- $\alpha$  and sTNFR2. However, there was no association with IR in this cohort, although a paracrine effect cannot be discounted. AFABP, an adipokine produced predominantly in adipocytes and macrophages (including hepatic Kupffer cells) with increased production in subcutaneous rather than visceral fat,<sup>46</sup> has been implicated in inflammation and IR in the metabolic syndrome and nonalcoholic fatty liver disease.<sup>47,48</sup> AFABP levels were nonsignificantly higher in CHC compared to controls. These data suggest that these adipocytokines may not have a major role in mediating the IR of CHC; however, it is interesting that AFABP is elevated and predictive of inflammation in nonalcoholic fatty liver disease,<sup>48</sup> while Lipocalin-2 is elevated in this infective form of liver disease.

Basal and clamp glucagon levels were elevated in CHC, a finding not described previously. We did not determine whether this was related to secretion or clearance, although hypersecretion has been suggested in hepatic cirrhosis. Elevated fasting glucagon has been associated with IR in nondiabetic populations<sup>49</sup> and attributed to IR of the pancreatic  $\alpha$ -cell; however, we did not show a relationship between clamp insulin action and glucagon in CHC. In this population, IR measured by HOMA-IR correlated poorly with clamp measures, but was strongly predicted by glucagon-to-insulin ratio, possibly reflecting greater influence of glucagon-to-insulin regulation on basal hepatic glucose output. However, glucagon levels did not correlate significantly with a basal hepatic insulin resistance index (EGP  $\times$  fasting insulin) and this index was similar in CHC and control subjects.

There were more smokers and methadone users among CHC subjects; however, we excluded these as confounding factors to IR. IR was similar in nonsmokers and smokers and, in fact, methadone users were more insulin-sensitive than nonusers, so methadone was clearly not a contributor to IR. As only Caucasian males were studied, these results cannot be applied to other ethnic groups or females without additional studies.

In summary, we have demonstrated for the first time that the IR of CHC, a unique infective/inflammatory paradigm of IR, is mainly in muscle; is independent of increased hepatic lipid (in genotype 3); and is coupled with elevated levels of glucagon and Lipocalin-2. The strong relationship with HCV viral load and subcutaneous (not visceral) fat suggests the possibility of a causative interplay between the virus and adipocyte, which will need to be further examined.

### Supplementary Material

Note: To access the supplementary material accompanying this article, visit the online version of *Gastroenterology* at [www.gastrojournal.org](http://www.gastrojournal.org), and at doi: [10.1053/j.gastro.2009.11.050](https://doi.org/10.1053/j.gastro.2009.11.050).

## References

1. Mehta SH, Brancati FL, Sulkowski MS, et al. Prevalence of type 2 diabetes mellitus among persons with hepatitis C virus infection in the United States. *Ann Intern Med* 2000;133:592–599.
2. Hui JM, Sud A, Farrell GC, et al. Insulin resistance is associated with chronic hepatitis C virus infection and fibrosis progression. *Gastroenterology* 2003;125:1695–1704.
3. Poustchi H, Negro F, Hui J, et al. Insulin resistance and response to therapy in patients infected with chronic hepatitis C virus genotypes 2 and 3. *J Hepatol* 2008;48:28–34.
4. Yazicioglu G, Isitan F, Altunbas H, et al. Insulin resistance in chronic hepatitis C. *Int J Clin Pract* 2004;58:1020–1022.
5. Vanni E, Abate ML, Gentilcore E, et al. Sites and mechanisms of insulin resistance in nonobese, nondiabetic patients with chronic hepatitis C. *Hepatology* 2009;50:697–706.
6. Bonora E, Targher G, Alberiche M, et al. Homeostasis model assessment closely mirrors the glucose clamp technique in the assessment of insulin sensitivity: studies in subjects with various degrees of glucose tolerance and insulin sensitivity. *Diabetes Care* 2000;23:57–63.
7. Nelson DR, Lim HL, Marousis CG, et al. Activation of tumor necrosis factor-alpha system in chronic hepatitis C virus infection. *Dig Dis Sci* 1997;42:2487–2494.
8. Shintani Y, Fujie H, Miyoshi H, et al. Hepatitis C virus infection and diabetes: direct involvement of the virus in the development of insulin resistance. *Gastroenterology* 2004;126:840–848.
9. Cua IH, Hui JM, Bandara P, et al. Insulin resistance and liver injury in hepatitis C is not associated with virus-specific changes in adipocytokines. *Hepatology* 2007;46:66–73.
10. Negro F. Insulin resistance and HCV: will new knowledge modify clinical management? *J Hepatol* 2006;45:514–519.
11. Hui JM, Kench J, Farrell GC, et al. Genotype-specific mechanisms for hepatic steatosis in chronic hepatitis C infection. *J Gastroenterol Hepatol* 2002;17:873–881.
12. Cheng Y, Dharancy S, Malapel M, et al. Hepatitis C virus infection down-regulates the expression of peroxisome proliferator-activated receptor alpha and carnitine palmitoyl acyl-CoA transferase 1A. *World J Gastroenterol* 2005;11:7591–7596.
13. Su AI, Pezacki JP, Wodicka L, et al. Genomic analysis of the host response to hepatitis C virus infection. *Proc Natl Acad Sci U S A* 2002;99:15669–15674.
14. Yki-Jarvinen H. Fat in the liver and insulin resistance. *Ann Med* 2005;37:347–356.
15. Lara-Castro C, Garvey WT. Intracellular lipid accumulation in liver and muscle and the insulin resistance syndrome. *Endocrinol Metab Clin North Am* 2008;37:841–856.
16. Sud A, Hui JM, Farrell GC, et al. Improved prediction of fibrosis in chronic hepatitis C using measures of insulin resistance in a probability index. *Hepatology* 2004;39:1239–1247.
17. Forn X, Ampurdanes S, Llovet JM, et al. Identification of chronic hepatitis C patients without hepatic fibrosis by a simple predictive model. *Hepatology* 2002;36:986–992.
18. Kannel WB, Sorlie P. Some health benefits of physical activity. The Framingham Study. *Arch Intern Med* 1979;139:857–861.
19. Australian Bureau of Statistics. 1995 National Nutrition Survey: User's Guide (4801.0). In: 3) FFQa, ed.
20. Scheuer PJ. Classification of chronic viral hepatitis: a need for reassessment. *J Hepatol* 1991;13:372–374.
21. Szczepaniak LS, Nurenberg P, Leonard D, et al. Magnetic resonance spectroscopy to measure hepatic triglyceride content: prevalence of hepatic steatosis in the general population. *Am J Physiol Endocrinol Metab* 2005;288:E462–E468.
22. Szczepaniak LS, Babcock EE, Schick F, et al. Measurement of intracellular triglyceride stores by H spectroscopy: validation in vivo. *Am J Physiol* 1999;276:E977–E989.
23. Positano V, Gastaldelli A, Sironi AM, et al. An accurate and robust method for unsupervised assessment of abdominal fat by MRI. *J Magn Reson Imaging* 2004;20:684–689.
24. Maggs DG, Buchanan TA, Burant CF, et al. Metabolic effects of troglitazone monotherapy in type 2 diabetes mellitus. A randomized, double-blind, placebo-controlled trial. *Ann Intern Med* 1998;128:176–185.
25. Moghetti P, Tosi F, Castello R, et al. The insulin resistance in women with hyperandrogenism is partially reversed by antiandrogen treatment: evidence that androgens impair insulin action in women. *J Clin Endocrinol Metab* 1996;81:952–960.
26. Wolfe RR. Radioactive and stable isotope tracers in biomedicine: principles and practice of kinetic analysis. New York, NY: Wiley-Liss, 1992.
27. Lusk G, Du Bois EF. On the constancy of the basal metabolism. *J Physiol* 1924;59:213–216.
28. Finegood DT, Bergman RN. Optimal segments: a method for smoothing tracer data to calculate metabolic fluxes. *Am J Physiol* 1983;244:E472–E479.
29. Steele R, Wall JS, De Bodo RC, et al. Measurement of size and turnover rate of body glucose pool by the isotope dilution method. *Am J Physiol* 1956;187:15–24.
30. Finegood DT, Bergman RN, Vranic M. Estimation of endogenous glucose production during hyperinsulinemic-euglycemic glucose clamps. Comparison of unlabeled and labeled exogenous glucose infusates. *Diabetes* 1987;36:914–924.
31. Hofer H, Bankl HC, Wrba F, et al. Hepatocellular fat accumulation and low serum cholesterol in patients infected with HCV-3a. *Am J Gastroenterol* 2002;97:2880–2885.
32. Hume R. Prediction of lean body mass from height and weight. *J Clin Pathol* 1966;19:389–391.
33. Aytug S, Reich D, Sapiro LE, et al. Impaired IRS-1/PI3-kinase signaling in patients with HCV: a mechanism for increased prevalence of type 2 diabetes. *Hepatology* 2003;38:1384–1392.
34. Kotronen A, Juurinen L, Tiikkainen M, et al. Increased liver fat, impaired insulin clearance, and hepatic and adipose tissue insulin resistance in type 2 diabetes. *Gastroenterology* 2008;135:122–130.
35. Mirandola S, Realdon S, Iqbal J, et al. Liver microsomal triglyceride transfer protein is involved in hepatitis C liver steatosis. *Gastroenterology* 2006;130:1661–1669.
36. Kraegen EW, Cooney GJ. Free fatty acids and skeletal muscle insulin resistance. *Curr Opin Lipidol* 2008;19:235–241.
37. Laskus T, Radkowski M, Wang LF, et al. Search for hepatitis C virus extrahepatic replication sites in patients with acquired immunodeficiency syndrome: specific detection of negative-strand viral RNA in various tissues. *Hepatology* 1998;28:1398–1401.
38. Kawaguchi T, Ide T, Taniguchi E, et al. Clearance of HCV improves insulin resistance, beta-cell function, and hepatic expression of insulin receptor substrate 1 and 2. *Am J Gastroenterol* 2007;102:570–576.
39. Moucari R, Asselah T, Cazals-Hatem D, et al. Insulin resistance in chronic hepatitis C: association with genotypes 1 and 4, serum HCV RNA level, and liver fibrosis. *Gastroenterology* 2008;134:416–423.
40. Gan SK, Kriketos AD, Poynten AM, et al. Insulin action, regional fat, and myocyte lipid: altered relationships with increased adiposity. *Obes Res* 2003;11:1295–1305.
41. Pittas AG, Joseph NA, Greenberg AS. Adipocytokines and insulin resistance. *J Clin Endocrinol Metab* 2004;89:447–452.

42. Whitehead JP, Richards AA, Hickman IJ, et al. Adiponectin—a key adipokine in the metabolic syndrome. *Diabetes Obes Metab* 2006;8:264–280.
43. Uysal KT, Wiesbrock SM, Marino MW, et al. Protection from obesity-induced insulin resistance in mice lacking TNF- $\alpha$  function. *Nature* 1997;389:610–614.
44. Hotamisligil GS. The role of TNF $\alpha$  and TNF receptors in obesity and insulin resistance. *J Intern Med* 1999;245:621–625.
45. Hoo RL, Yeung DC, Lam KS, et al. Inflammatory biomarkers associated with obesity and insulin resistance: a focus on Lipocalin-2 and adipocyte fatty acid-binding protein. *Expert Rev Endocrinol Metab* 2008;3:29–41.
46. Fisher RM, Thorne A, Hamsten A, et al. Fatty acid binding protein expression in different human adipose tissue depots in relation to rates of lipolysis and insulin concentration in obese individuals. *Mol Cell Biochem* 2002;239:95–100.
47. Furuhashi M, Hotamisligil GS. Fatty acid-binding proteins: role in metabolic diseases and potential as drug targets. *Nat Rev Drug Discov* 2008;7:489–503.
48. Milner KL, van der Poorten D, Xu A, et al. Adipocyte fatty acid binding protein levels relate to inflammation and fibrosis in non-alcoholic fatty liver disease. *Hepatology* 2009;49:1926–1934.
49. Ferrannini E, Muscelli E, Natali A, et al. Association of fasting glucagon and proinsulin concentrations with insulin resistance. *Diabetologia* 2007;50:2342–2347.

---

Received May 4, 2009. Accepted November 20, 2009.

#### *Reprint requests*

Address requests for reprints to: Donald Chisholm, MBBS, FRACP, Diabetes and Obesity Program, Garvan Institute of Medical Research, 384 Victoria Street, Darlinghurst, NSW 2010, Australia. e-mail: [d.chisholm@garvan.org.au](mailto:d.chisholm@garvan.org.au); fax: (61) 2 9295 8201.

#### *Acknowledgments*

Drs George and Chisholm contributed equally to this work and are joint senior authors.

Clinical trials registry no: NCT00707603.

#### *Conflicts of interest*

The authors disclose no conflicts.

#### *Funding*

Supported by grants from the National Health and Medical Research Council of Australia (Grant 358398), GESA postgraduate medical research scholarship, Robert W. Storr Bequest to the University of Sydney, a University of Sydney Grant and Hong Kong Research Council CRF (HKU 2/07C to A.X.). K.M. is supported by a National Health and Medical Research Council Postgraduate scholarship. M.T. is supported by a Diabetes UK RD Lawrence Fellowship.

## Supplementary Materials and Methods

### Subjects

Twenty-nine male, nonobese (BMI  $25.7 \pm 0.6$ ) Caucasian subjects (median age, 40 years; range, 29–53 years) with CHC (the majority with injecting drug use acquired infection) genotype 1 ( $n = 15$ ) or 3 ( $n = 14$ ), due to start antiviral therapy at 4 different hospital clinics were recruited to the study between 2005 and 2008. To minimize the impact of known determinants of insulin resistance, inclusion criteria included (1) BMI  $<30$ , (2) fasting blood glucose level  $<5.5$ , (3) absent or minimal fibrosis (fibrosis score  $\leq F2$ ) on liver biopsy (23 subjects [79%] had a liver biopsy) or a Fibrosis Probability Index score<sup>1</sup>  $\leq 0.3$  and Forns index<sup>2</sup>  $<6.9$  d), (4) male gender, and (5) Caucasian background. Fifteen healthy HCV antibody–negative controls recruited from the community (median age, 37 years) with normal liver function tests were matched by age, ethnicity, gender, and BMI to these subjects. Patients with alcohol consumption  $>20$  g per day were excluded (assessed by 2 separate interviews with the patient and family members). Other exclusion criteria included concurrent HIV or other causes of liver disease. This study had 80% power to detect a difference in glucose infusion rate (measure of IR) of  $3 \text{ mg} \cdot \text{kg}^{-1} \cdot \text{min}^{-1}$  between groups containing 15 subjects each, assuming a common standard deviation of 2.8. All examinations were undertaken following a 10-hour fast with following abstinence of strenuous exercise and alcohol or use of addictive drugs for 48 hours prior to the study. Those on methadone could continue their normal dosing regime. Routine physical activity (exercise/home duties) was assessed by a standardized validated questionnaire (Framingham Physical Activity Index)<sup>3</sup> calculating average weekly energy expenditure in metabolic units. Dietary composition and energy intake were measured by a detailed dietary history based on 24-hour recall<sup>4</sup> (Australian Bureau of Statistics 1995 National Nutrition Survey: User's Guide, 4801.0) and quantification using a standard food composition program (FoodWorks; Xyris Software, Brisbane, Australia). The protocols were approved by the Institutional Human Research Ethics Committee and all subjects provided written informed consent.

### Histopathology

Twenty-three subjects had a liver biopsy as part of the CHC management. The degree of necroinflammatory activity and fibrosis were scored semi-quantitatively as described by Scheuer.<sup>5</sup> Portal or periportal and lobular inflammatory activity were scored from 0 to 4. Fibrosis was scored as follows: F0, no fibrosis; F1, enlarged fibrotic portal tracts; F2, periportal or portal-portal septa, but intact architecture.

### Magnetic Resonance Spectroscopy and Imaging

All magnetic resonance examinations were undertaken on a 1.5-Tesla scanner (General Electric Medical Systems, Milwaukee, WI). Image localized water suppressed and unsuppressed  $^1\text{H}$ -magnetic resonance spectra were collected from a  $1.5 \times 1.5 \times 2 \text{ cm}^2$  voxel within the soleus muscle avoiding blood vessels and fatty tissue. Spectra were collected using a 10-cm  $^1\text{H}$  tuned surface coil around the right calf (General Electric Medical Systems) and a PRESS pulse sequence (repetition time [TR] = 5000 ms and echo time [TE] = 32 ms, 32 averages).

### Liver $^1\text{H}$ -Magnetic Resonance Spectroscopy

Image localized  $^1\text{H}$ -MR spectra of the liver were obtained using a  $12 \times 14 \text{ cm}^2$   $^1\text{H}$  tuned butterfly  $^1\text{H}$  coil (General Electric Medical Systems) placed over the lateral aspect of the abdomen. Spectra were collected from a  $2 \times 2 \times 2 \text{ cm}^3$  voxel avoiding blood vessels, ducts, and fat tissue using a modified PRESS pulse sequence (TR = 1500 ms, TE = 125 ms, 12 averages).

### Analysis of Magnetic Resonance Spectra

Interpretation of  $^1\text{H}$ -magnetic resonance spectra was performed with the java-based magnetic resonance user interface (JMRUI version 2.0)<sup>6</sup> using the AMARES algorithm.<sup>7</sup> Intramyocellular lipid concentrations were calculated as described previously.<sup>8</sup> Hepatic lipid content was calculated as described previously<sup>9</sup> and expressed relative to water content of the liver (ratio of signal from fat [f] to total signal from fat and water [w]) ( $f/(f + w)$  %).

### Abdominal Fat Determinations

Five  $T_1$ -weighted axial magnetic resonance images (10-mm thick, 2-mm gap) were collected during a breath-hold at the level of the 4th lumbar vertebra. Images were analyzed using HIPPO FAT software for determination of abdominal subcutaneous and visceral adipose tissue areas.<sup>10,11</sup> Fat volumes were multiplied by a factor of 0.92<sup>12</sup> to calculate their mass in kilograms.

### Baseline Assessment and Anthropometry

Following imaging, all subjects had a complete clinical and anthropometric investigation. Weight, height, and waist circumference (midpoint between the lower border of the rib cage and the iliac crest) were measured, and BMI was calculated as weight (in kg) divided by height squared ( $\text{m}^2$ ) and waist-to-hip ratio by dividing waist circumference by hip circumference. Blood pressure was measured in the supine position after a 5-minute rest using a mercury sphygmomanometer. Teflon catheters were placed in the antecubital vein for infusions and into a contralateral dorsal hand vein, heated using a warming device placed over the arm and hand to achieve arterialization of venous blood, for blood sampling. A small volume of normal saline (0.9%) was infused in both lines

to maintain patency. Blood was collected for plasma insulin, glucose, lipids, highly sensitive C-reactive protein, adiponectin, liver function tests, glucagon, c-peptide, leptin, TNF- $\alpha$ , sTNFR2, nonesterified free fatty acids, AFABP, Lipocalin-2, and IL-6.

### ***Intravenous Glucose Tolerance Test (IVGTT)***

An IVGTT was performed to assess B-cell dysfunction as a potential contributor to type 2 diabetes in CHC. A bolus of 50% dextrose (300 mg/kg, maximum, 24 g) was administered intravenously for 1 minute through an antecubital vein with blood sampling for glucose (YSI 2300 Stat Plus, Yellow Springs Instruments, Yellow Springs, OH) and insulin levels at 1, 3, 5, 7, and 10 minutes. The acute insulin response was calculated as the ratio of the increment of serum insulin (mU/L) to that of blood glucose (mmol/L) during the 10 minutes of the IVGTT. The incremental insulin (AUC<sub>insulin</sub>) and glucose (AUC<sub>glucose</sub>) areas under the curve were calculated by the trapezoidal method.

### ***Hyperinsulinemic-Euglycemic Clamp***

A 2-hour primed (5 mg · kg<sup>-1</sup> body weight) continuous infusion (3 mg · kg<sup>-1</sup> · h<sup>-1</sup>) of [6,6-<sup>2</sup>H] glucose (Cambridge Isotope Laboratories, Andover, MA, USA) was begun through an antecubital vein. Blood samples were withdrawn at 10-minute intervals during the final 30 minutes of the 2nd hour for the measurement of plasma glucose, insulin levels, and glucose isotope enrichment. After this, a 2-step hyperinsulinemic-euglycemic clamp was initiated as described previously.<sup>13,14</sup> During the first step a low dose of insulin (60 U Actrapid HM, Novo Nordisk, Copenhagen, Denmark in 500 mL normal saline) was infused at 15 mU · m<sup>-2</sup> · min<sup>-1</sup> for 90 minutes. During the second step a priming dose of insulin was administered followed by a high continuous dose of insulin at 80 mU · m<sup>-2</sup> · min<sup>-1</sup> for 120 minutes to assess insulin's effects on peripheral glucose disposal (this dose has been shown to suppress endogenous glucose production<sup>14</sup> even in the presence of moderate insulin resistance; therefore, the amount of glucose infused is equivalent to peripheral glucose disposal). The plasma glucose level (by YSI) was maintained at 5 mmol/L with a variable-rate infusion of dextrose (25 g/100 mL enriched to approximately 2.5% with di-deuterated glucose) adjusted according to 10-minute results. The steady-state glucose infusion rate (M value) represented the whole-body glucose disposal rate, an estimate of insulin sensitivity, and was calculated as a mean at 10-minute intervals during the last 40 minutes of the low-dose and high-dose insulin clamp. Five subjects (3 controls and 2 CHC subjects) did not receive this enhanced [6,6-<sup>2</sup>H<sub>2</sub>] glucose delivery during hyperinsulinemia and are not included in glucose turnover studies during the hyperinsulinemia, although basal turnover and clamp glucose infusion rate are reliable and included in the results. One

control subject did not attain steady state during low dose insulin. Thus numbers for basal glucose turnover data are control 15, CHC 29. For the clamp low dose insulin (and for calculations of low insulin vs basal), the numbers are control 11, CHC 27. The coefficient of variation for the glucose levels at the low- and high-dose insulin was 2.66% and 3.98%, respectively. Glucose levels achieved in the hepatitis C subjects and controls during the low dose insulin were 4.9 ± 0.02 vs 4.8 ± 0.1 mmol/L, *P* = .1 and at high-dose insulin 5 ± 0.03 vs 5 ± 0.06 mmol/L; *P* = .99, respectively. Blood samples were also drawn at these intervals for insulin, glucagon (frozen with trasylol), c-peptide, and glucose isotope enrichment. On conclusion of the clamp, subjects received a meal and glucose was continued for a further 30 minutes until blood glucose stabilized. Blood samples were immediately cold-centrifuged at +4°C. Serum was stored at -80°C until analyses.

### ***Calorimetry***

During the final 30 minutes of the basal infusion and each step of the clamp, indirect calorimetry was performed using the ventilated hood technique (Deltatrack Metabolic Monitor; Datex Instrumentarium, Helsinki, Finland) to measure basal fasting and insulin stimulated glucose and fat oxidation as described previously.<sup>15</sup> An equilibrium period of 10 minutes was allowed (data excluded from calculations), after which gas exchange rates were recorded at minute intervals; energy expenditure and respiratory quotient (ratio of carbon dioxide production to oxygen consumption) were then calculated.<sup>16</sup> Subjects were discouraged from talking, coughing, sneezing, or sleeping for the duration of this period. Nonoxidative glucose metabolism was calculated as whole-body glucose disposal rate minus glucose oxidation rate.

### ***Analyses***

Commercial radioimmunoassays (LincoResearch, Inc, St. Charles, MO) were used to analyze serum insulin, glucagon, adiponectin, and c-peptide. Leptin, TNF- $\alpha$ , sTNFR2, and IL-6 were measured in duplicate using enzyme-linked immunosorbent assays (Diagnostic Systems Laboratories, Webster, TX and Quantikine ELISA; R&D Systems, Minneapolis, MN). Nonesterified free fatty acids were measured by an enzymatic colorimetric method (NEFA C, Wako Chemicals GmbH, Neuss, Germany). Highly sensitive C-reactive protein was measured by a highly sensitive Near Infrared Particle Immunoassay (Beckman Coulter Synchron LX system Chemistry analyzer, CV 2.2%–3.7%). Serum AFABP and Lipocalin-2 were measured with immunoassays as we described previously.<sup>17,18</sup> The intra- and interassay coefficient of variations for A-FABP were 3.7%–6.4% and 2.6%–5.3%, respectively. The intra- and interassay coefficient of variations for Lipocalin-2 were 3.8%–6.0% and 3.1%–5.2%, respectively. Lipid and liver function tests were per-

formed using a conventional automated analyzer within the Department of Clinical Chemistry at St Vincent's Hospital. Gas chromatography-mass spectrometry (Agilent Technologies 6890 gas chromatograph interfaced to an Agilent 5973 Mass Selective Detector; Agilent Technologies, Ryde, NSW, Australia) analysis of enrichments of [6,6-<sup>2</sup>H] glucose in plasma and infusates were performed with the gas chromatography-mass spectrometry in positive ion chemical ionization mode using the pentaacetate derivative of glucose by selectively monitoring ions at *m/z* 328 and 330 for moles percent enrichment in glucose.<sup>19</sup> The coefficient of variation for deuterated glucose measurements at the low- and high-dose insulin was 4.8% and 3.7%, respectively. Viral load or HCV RNA was measured by the polymerase chain reaction method (Amplicor HCV; Roche Diagnostics, Branchburg, NJ) and HCV antibodies (Monolisa anti-HCV; Sanofi Diagnostics Pasteur, Marnes-la-Coquette, France) were measured using enzyme-linked immunoassay (Beckman method). HCV genotype was performed using a second generation reverse hybridization probe assay (inno-Lipa HCV II; Immunogenetics, Zwijndrecht, Belgium).

### Calculations

Isotopic enrichment determined by gas chromatography-mass spectrometry was corrected for the constant background contribution of naturally occurring [6,6-<sup>2</sup>H<sub>2</sub>] glucose, and the values obtained were smoothed by linear regression against time within each measurement period.<sup>20</sup> The rates of EGP and TGD were estimated during the basal and insulin-stimulated 30-minute steady-state periods using Steele's 1-compartment fixed-volume model (assuming a pool-fraction of 0.65 and a volume of distribution of 20% of body weight),<sup>21</sup> as modified by Finegood et al<sup>22</sup> to account for the added infusion of labeled exogenous glucose.

### Supplementary References

- Sud A, Hui JM, Farrell GC, et al. Improved prediction of fibrosis in chronic hepatitis C using measures of insulin resistance in a probability index. *Hepatology* 2004;39:1239–1247.
- Forns X, Ampurdanes S, Llovet JM, et al. Identification of chronic hepatitis C patients without hepatic fibrosis by a simple predictive model. *Hepatology* 2002;36:986–992.
- Kannel WB, Sorlie P. Some health benefits of physical activity. The Framingham Study. *Arch Intern Med* 1979;139:857–861.
- Australian Bureau of Statistics. 1995 National Nutrition Survey: User's Guide (4801.0). In: 3) FFQa, ed.
- Scheuer PJ. Classification of chronic viral hepatitis: a need for reassessment. *J Hepatol* 1991;13:372–374.
- Narressi A, Couturier C, Castang I, et al. Java-based graphical user interface for MRUI, a software package for quantitation of in vivo/medical magnetic resonance spectroscopy signals. *Comput Biol Med* 2001;31:269–286.
- Vanhamme L, Van Huffel S, Van Hecke P, et al. Time-domain quantification of series of biomedical magnetic resonance spectroscopy signals. *J Magn Reson* 1999;140:120–130.
- Szczepaniak LS, Babcock EE, Schick F, et al. Measurement of intracellular triglyceride stores by H spectroscopy: validation in vivo. *Am J Physiol* 1999;276:E977–E989.
- Szczepaniak LS, Nurenberg P, Leonard D, et al. Magnetic resonance spectroscopy to measure hepatic triglyceride content: prevalence of hepatic steatosis in the general population. *Am J Physiol Endocrinol Metab* 2005;288:E462–E468.
- Positano V, Gastaldelli A, Sironi AM, et al. An accurate and robust method for unsupervised assessment of abdominal fat by MRI. *J Magn Reson Imaging* 2004;20:684–689.
- Demerath EW, Ritter KJ, Couch WA, et al. Validity of a new automated software program for visceral adipose tissue estimation. *Int J Obes (Lond)* 2007;31:285–291.
- Snyder W, Cooke M, Mnasset E, et al. Report of the task group on reference man. Oxford, UK: Pergamon, 1975.
- Maggs DG, Buchanan TA, Burant CF, et al. Metabolic effects of troglitazone monotherapy in type 2 diabetes mellitus. A randomized, double-blind, placebo-controlled trial. *Ann Intern Med* 1998;128:176–185.
- Moggetti P, Tosi F, Castello R, et al. The insulin resistance in women with hyperandrogenism is partially reversed by antiandrogen treatment: evidence that androgens impair insulin action in women. *J Clin Endocrinol Metab* 1996;81:952–960.
- Lusk G, Du Bois EF. On the constancy of the basal metabolism. *J Physiol* 1924;59:213–216.
- Ferrannini E. The theoretical bases of indirect calorimetry: a review. *Metabolism* 1988;37:287–301.
- Xu A, Wang Y, Xu JY, et al. Adipocyte fatty acid-binding protein is a plasma biomarker closely associated with obesity and metabolic syndrome. *Clin Chem* 2006;52:405–413.
- Wang Y, Lam KS, Kraegen EW, et al. Lipocalin-2 is an inflammatory marker closely associated with obesity, insulin resistance, and hyperglycemia in humans. *Clin Chem* 2007;53:34–41.
- Wolfe RR. Radioactive and stable isotope tracers in biomedicine: principles and practice of kinetic analysis. New York, NY: Wiley-Liss, 1992.
- Finegood DT, Bergman RN. Optimal segments: a method for smoothing tracer data to calculate metabolic fluxes. *Am J Physiol* 1983;244:E472–E4729.
- Steele R, Wall JS, De Bodo RC, et al. Measurement of size and turnover rate of body glucose pool by the isotope dilution method. *Am J Physiol* 1956;187:15–24.
- Finegood DT, Bergman RN, Vranic M. Estimation of endogenous glucose production during hyperinsulinemic-euglycemic glucose clamps. Comparison of unlabeled and labeled exogenous glucose infusates. *Diabetes* 1987;36:914–924.